International Journal of Computer Information Systems and Industrial Management Applications
ISSN 2150-7988 Volume 17 (2025) pp. 1-16

https://doi.org/10.70917/ijcisim-2025-0251
Article

Research on the influence mechanism of virtual reality technology on pilots' balance perception ability training

Wei Song [1,*] and Li'na Wang [2]

[1] Physical Education Department, Civil Aviation University of China, Tianjin, 300300, China
[2] Department of Physical Education, Tiangong University, Tianjin, 300387, China; 1984renwofei@163.com

Abstract: In this paper, the differential equations of the six-degree-of-freedom motion of a rigid-body vehicle in the presence of wind perturbation are derived, and a virtual cockpit 3D model and human balance perception ability detection system are designed. Through theoretical modeling, platform implementation and empirical testing, the influence mechanism of virtual reality technology on pilots' balance perception ability is deeply analyzed. The mean data obtained from the reaction time test decreased by 49.3s in the experimental group and 18.5s in the control group after the experiment, and the independent sample t-test between the groups yielded a p-value of 0.024, which is a significant difference. The mean value of the number of correct tests per unit of time in the experimental group after training increased by 0.017 per second, and the control group increased by 0.006 per second, and the p-value of the independent samples T-test between the groups was 0.019, which is also a significant difference. Virtual reality technology strengthens the development of neuroplasticity of balance perception in pilots through highly immersive scene simulation with multimodal sensory synchronized feedback, which can significantly improve balance perception.

Keywords: virtual reality technology; virtual cockpit; balance perception ability; pilots

1. Introduction

In recent years, with the rapid development of simulation technology and computer technology, the development of virtual reality (VR) technology has also soared, just like it has become a popular research direction in various universities and research institutions. VR technology is a high-tech, which is based on the core of computer graphic display technology, and establishes a virtual environment model through the three-dimensional data of a certain range of environment [1-3]. In the simulation system, a highly realistic visual, auditory, tactile and even olfactory virtual environment is generated. Users use some necessary hardware devices (e.g., helmet displays, data gloves, force sensing devices, etc.) to interact and interact with objects in the virtual environment, and are able to experience highly realistic three-dimensional visual sensations [4]. Flight training simulation is a ground-based flight simulation device with exactly the same cockpit equipment and maneuvering equipment as a real aircraft, where the pilot receives various flight information generated by the flight simulation system in the cockpit, and operates and controls the aircraft system through judgment and decision-making [5-7]. Using VR technology to simulate the flight simulator's maneuvering system, view system and other simulations can greatly improve the trainee's real sense of immersion and significantly improve training efficiency [8]. At the same time, the task of different models and different simulation functions can be realized by changing the software and database, reducing the cost of research and development and flight training.

With the rapid development of computer vision technology, vision-based interaction solutions can better reflect the "human-centered" interaction characteristics, and gradually become a research hotspot in the field of VR interaction. Literature [9] developed a virtual reality flight simulator (VR-FS), which integrates human-machine interface (HMI) and human factors engineering (HF), and the use of flight simulators for training can reduce the expenditure of resources and training costs, and in the simulation

phase of the flight can be very good practice of the basic maneuvering skills of the trainee, the basic state of the interchanges and the allocation of attention and other key points. Literature [10] provides a systematic review of the key elements of visual scenarios, motion and sound simulation in flight simulation training, and the main goal of this technology is to provide pilots with a virtual flight environment, where the whole process involves human sensory, perceptual and cognitive functions. Literature [11] explored the application of VR in flight simulation, and found that compared to traditional simulators, the use of VR technology for simulation of the flight simulator's maneuvering system, visual scene system and other simulations can greatly improve the trainee's sense of real immersion, and significantly improve the training efficiency. Literature [12] proposed to provide P1135 flight simulation equipment to build an experimental platform in order to train pilots' mental load, flight operation performance, resilience and response in different flight situations, and successfully simulated the scenarios of normal flight, single-failure flight and multi-failure flight. Literature [13] utilized a VR headset combined with a flight simulator (FGFS) and applied it to flight simulation training, and found that the technology can enhance the thinking ability available to pilots when completing assigned tasks, as well as improve pilots' situational awareness, enabling pilots to complete a large number of real-world flight tests in a simulated environment using the same data transfer procedures. Literature [14] proposes the use of Extended Reality (XR) technology as an alternative to traditional flight simulators and airplanes, aiming to save pilots training time and money while also improving training effectiveness, and evidence from a systematic review suggests that there is great potential for the use of this technology in flight training.

A systematic review of existing research on VR-based flight simulators in the literature [15] found that much of the existing research has focused on the training of individual users on small piston aircraft, while relatively little has been done on flight training for commercial pilots. Literature [16] constructed a pilot simulation training system based on VR technology that combines a visualization simulation system with a control algorithm simulation system, which implements a three-dimensional model and adds and establishes simulation environments and special effects to achieve the study and improvement of its interactive control model. Literature [17] compared two pilot training methods, Physical Flight Simulator (PFS) and VR-FS, and found that PFS is disadvantageous because of very high acquisition and operational costs, while VR-FS can be a cost-effective and flexible alternative, and pilots are inferior to PFS in terms of task completion time, simulator discomfort, and psychological demands when training under VR-FS. Literature [18] explored the use of VR technology in flight simulation training with 120 junior instrument pilots and found that the advantages of the technology were the highly realistic environment, the high degree of fit with the real world, and the low cost. Literature [19] explored the Canadian general aviation industry pilots, for the use of Flight Simulation Training Devices (FSTD) combined with Augmented Reality (AR) technology, and found that in concert with AR, pilots showed a strong interest in flight training, while the immersive, technology-driven training environment also helped to improve the pilots' skill levels.

Pilot's balance perception ability is a core element to ensure flight safety, which integrates multi-sensory information such as vision, vestibular sense and proprioception to help pilots accurately judge their own position and movement status in three-dimensional space [20]. This ability is especially important in high-altitude and high-speed environments, because the mismatch between the sensory system and the flight environment may lead to spatial orientation obstacles, which in turn may cause safety risks. Currently, studies on the application of immersive technologies such as VR in flight simulation training have demonstrated the advantages of these technologies in pilot training, however, the mechanism of the effect of VR on the balance perception ability of pilots needs to be further investigated.

This paper firstly elaborates the theory of aircraft motion modeling and the six-degree-of-freedom equations, and introduces the definition of multiple types of coordinate systems, such as airframe, stability, velocity, and trajectory. Based on the open-source platform FlightGear, the construction of virtual cockpit system is realized by combining AC3D modeling and communication programs. Design the experimental platform for testing the pilot's balance perception ability, and detail its specific implementation program. Verify the accuracy of the proposed system through flight cockpit tracking performance tests. Carry out balance perception ability assessment based on pilot groups, and analyze the difference characteristics between different spatial abilities and gender groups. Combined with the comparative experimental data, the influence path of virtual reality technology on balance perception ability is explored.

2. Design and realization of a flight simulation platform based on virtual reality technology

With the rapid development of civil aviation, there is an urgent demand for a large number of high-quality and high-level pilots. However, the traditional pilot training method has a long cycle, large investment and high risk, therefore, it is of great practical significance to research and develop a set of efficient, safe and economical pilot training system. As the core foundation of pilot's spatial orientation and attitude control, balance perception ability directly affects flight safety and mission performance. In recent years, virtual reality technology has shown a broad application prospect in the field of pilot training due to its high immersion, strong interactivity and flexibility in scene construction.

2.1. Body motion modeling

2.1.1. Coordinate system

The motion of the vehicle must be described within a coordinate system, and by convention, all coordinate systems used in this paper are right-handed orthogonal coordinate systems.

(1) Ground coordinate system OgXgYgZg

Fixed on the ground surface, the origin is located at any selected point on the ground, the Xg axis points to any fixed direction on the ground plane, the Zg axis is plumbed down, and the Yg axis is perpendicular to the OgXgZg plane pointing to the right. This coordinate system is generally regarded as an inertial system.

(2) Body coordinate system ObXbYbZb

The origin is located in the center of mass of the vehicle, Xb axis is located in the plane of symmetry of the vehicle, parallel to the axis of the fuselage pointing forward; Zb axis is located in the plane of symmetry, perpendicular to the Xb axis, pointing down; Yb axis is perpendicular to the ObXbZb plane, pointing to the right.

(3) Stabilized coordinate system OsXsYsZs

The origin is located in the center of mass of the vehicle, Xs axis is taken as the projection direction of the unperturbed flight speed in the symmetry plane, Zs axis is in the symmetry plane, perpendicular to the Xs axis, pointing downward, Ys axis is perpendicular to the symmetry plane, pointing to the right.

(4) Velocity coordinate system OaXaYaZa

The origin is located in the center of mass of the vehicle, Xa axis points to the direction of airspeed; Za axis is located in the symmetry plane, perpendicular to the Xa axis downward; Ya axis is perpendicular to the OaXaZa plane, pointing to the right.

(5) Trajectory coordinate system OkXkYkZk

The origin is located in the center of mass of the vehicle, the Xk axis points to the direction of ground speed; the Zk axis is located in the plumb plane containing the Xk axis, perpendicular to the Xk axis downward; the Yk axis is perpendicular to the OkXkZk plane, pointing to the right.

2.1.2. Basic equations of motion for a rigid-body vehicle with six degrees of freedom

Before establishing the equations of motion of the vehicle, the following assumptions are made:

The vehicle is a rigid body with a symmetrical left-right distribution of mass, and the effects of movable parts on the vehicle are neglected.

The rotation of the earth and the curvature of the ground are neglected, and the ground coordinate system is regarded as an inertial system.

The rotational effect of engine rotation is not counted.

The center of mass of the vehicle is kept constant during the simulation.

The mass of the vehicle is constant during the simulation.

Under the above assumptions, according to Newton's second law, the differential equation of the vehicle translational dynamics is:

$$\vec{F} = \frac{d}{dt}\left(m\vec{V}_g\right)\Big|_g \tag{1}$$

where $\vec{F} = \vec{R} + \vec{P} + \vec{G}$ is the combined force vector of all external forces, $\vec{R}$ is the aerodynamic force vector, $\vec{P}$ is the engine thrust vector, and $\vec{P} = T\begin{bmatrix} T\cos i_e \\ 0 \\ -T\sin i_e \end{bmatrix}_m$, where T is the engine thrust and

i_e is the engine mounting angle. $\vec{G}$ is the gravity vector, $\vec{G}=\left(G_x,G_y,G_z\right)=\begin{bmatrix}-mg\sin\theta\\ mg\sin\phi\cos\theta\\ mg\cos\phi\cos\theta\end{bmatrix}$. m is vehicle mass. $\vec{V}_g$ is the velocity vector of the vehicle in the inertial system.

Let the ground inertial system be OgXgYgZg, the active coordinate system with the origin at the center of mass of the vehicle be OmXmYmZm, and the absolute velocity vector of the moving coordinate system relative to the ground inertial coordinate system be $\vec{V}_g$, and the rotational angular velocity vector be $\vec{\omega}$. An example of the inertial and kinematic coordinate systems is shown in Figure 1.

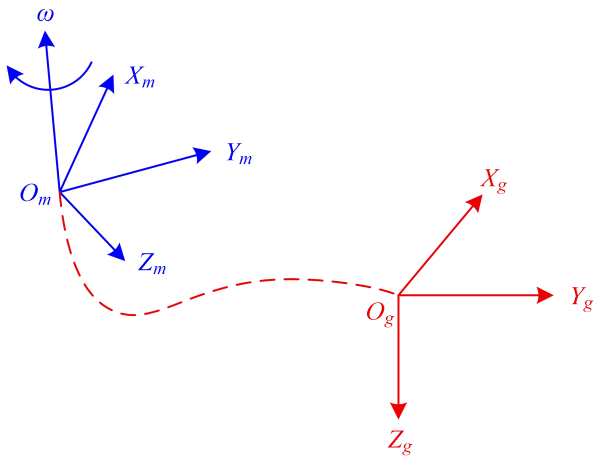

Figure 1. Inertial coordinate system and motion coordinate system.

Then the equations for the center of mass dynamics in vector form can be obtained as:

$$\vec{F}=\frac{d}{dt}\left(m\vec{V}_g\right)\Big|_m+\vec{\omega}\times\left(m\vec{V}_g\right) \tag{2}$$

Decompose the vector in the above equation along the three axes of the moving coordinate system OmXmYmZm:

$$\vec{V}_g=\left(u_m,v_m,w_m\right) \tag{3}$$

$$\vec{F}=\left(F_x,F_y,F_z\right) \tag{4}$$

$$\vec{\omega}=(p,q,r) \tag{5}$$

$$\vec{R}=\left(R_x,R_y,R_z\right) \tag{6}$$

Then there is:

$$\begin{aligned}F_x&=m\left(\dot{u}_m+qw_m-rv_m\right)=R_x+T\cos i_e-mg\sin\theta\\ F_y&=m\left(\dot{v}_m+ru_m-pw_m\right)=R_y+mg\cos\phi\cos\theta\\ F_z&=m\left(\dot{w}_m+pv_m-qu_m\right)=R_y-T\sin i_e+mg\cos\phi\sin\theta\end{aligned} \tag{7}$$

When the moving coordinate system is the body coordinate system ObXbYbZb, the above equation can be written as:

$$\begin{aligned}F_x&=m\left(\dot{u}_b+qw_b-rv_b\right)=R_x+T\cos i_c-mg\sin\theta\\ F_y&=m\left(\dot{v}_b+ru_b-pw_b\right)=R_y+mg\cos\phi\cos\theta\\ F_z&=m\left(\dot{w}_b+pv_b-qu_b\right)=R_y-T\sin i_c+mg\cos\phi\sin\theta\end{aligned} \tag{8}$$

Or:

$$\begin{aligned}\dot{u}_b &= \frac{R_x + T\cos i_e - mg\sin\theta}{m} - qw_b + rv_b \\ \dot{v}_b &= \frac{R_y + mg\cos\phi\cos\theta}{m} - ru_b + pw_b \\ \dot{w}_b &= \frac{R_y - T\sin i_e + mg\cos\phi\sin\theta}{m} - pv_b + qu_b\end{aligned} \tag{9}$$

$\vec{V}_g$ is represented in the ground coordinate system $\mathrm{O}_g\mathrm{X}_g\mathrm{Y}_g\mathrm{Z}_g$ as $\vec{V}_g = \left(u_g, v_g, w_g\right)$, and in the body coordinate system $\mathrm{O_bX_bY_bZ_b}$ it is expressed as: $\vec{V}_g = \left(u_b, v_b, w_b\right)$. Then we have: $\begin{bmatrix} u_g \\ v_g \\ w_g \end{bmatrix} = L_{gb}\begin{bmatrix} u_b \\ v_b \\ w_b \end{bmatrix}$, where $L_{gb} = L_{bg}^T$ is the transformation matrix from the airframe coordinate system to the ground coordinate system:

$$L_{gb} = \begin{bmatrix} \cos\theta\cos\psi & \sin\theta\sin\phi\cos\psi - \cos\phi\sin\psi & \sin\theta\cos\phi\cos\psi + \sin\phi\sin\psi \\ \cos\theta\sin\psi & \sin\theta\sin\phi\sin\psi + \cos\theta\cos\psi & \sin\theta\cos\phi\sin\psi - \sin\phi\cos\psi \\ -\sin\theta & \cos\theta\sin\phi & \cos\theta\cos\phi \end{bmatrix} \tag{10}$$

The relation between $\vec{V}_g$ and the heading angle and track inclination is:

$$\begin{aligned} V_g &= \sqrt{u_g^2 + v_g^2 + w_g^2} \\ u_g &= V_g\cos\gamma\cos\chi \end{aligned} \tag{11}$$

$$\begin{aligned} v_g &= V_g\cos\gamma\sin\chi \\ w_g &= -V_g\sin\gamma \end{aligned} \tag{12}$$

$$\begin{aligned} \chi &= \tan^{-1}\left(\frac{u_g}{v_g}\right) \\ \gamma &= -\sin^{-1}\left(\frac{w}{V_g}\right) \end{aligned} \tag{13}$$

Easily accessible:

$$\frac{dV_g}{dt} = \frac{\left(u_g\dot{u}_g + v_g\dot{v}_g + w_g\dot{w}_g\right)}{V_g} \tag{14}$$

$$\frac{d\chi}{dt} = \frac{u_g\dot{v}_g - v_g\dot{u}_g}{u_g^2 + v_g^2} \tag{15}$$

$$\frac{d\gamma}{dt} = \frac{V_g\dot{w}_g - w_g\dot{V}_g}{V_g^2\cos\gamma} \tag{16}$$

The differential equations for the rotational dynamics of the vehicle can be obtained from the momentum moment theorem:

$$\vec{M} = \frac{d}{dt}\vec{H}\bigg|_g \tag{17}$$

$$\vec{M} = (\bar{L}, \bar{M}, \bar{N}) = \vec{M}_a + \vec{M}_p \tag{18}$$

where $\vec{M}$ is the combined moment vector of all moments. $\vec{M}_a$ is the aerodynamic moment vector. $\vec{M}_p$ is the moment vector generated by the thrust vector, $\vec{M}_p = T\begin{bmatrix} -Y_e \sin i_e \\ Z_e \cos i_e \\ -Y_e \cos i_e \end{bmatrix}_m$. $\vec{H}$ is the angular momentum (momentum moment) vector.

There are in the kinetic coordinate system:

$$\vec{M} = \frac{d}{dt}\vec{H}\bigg|_m + \omega \times \vec{H} \tag{19}$$

The lemniscate tensor of the vehicle, Zhiku, is denoted as $I = \begin{bmatrix} I_x & -I_{xy} & -I_{xz} \\ -I_{yx} & I_y & -I_{yz} \\ -I_{xx} & -I_{zy} & I_z \end{bmatrix}_m$ in the dynamic coordinate system, and for symmetric vehicles there is $I_{xy} = I_{zy} = 0$. Substituting $\vec{H} = I\vec{\omega} = \begin{bmatrix} I_x p - I_{xx} r \\ I_y q \\ I_z r - I_{xz} p \end{bmatrix}$ into the previous equation yields:

$$\begin{bmatrix} \dot{p} \\ \dot{q} \\ \dot{r} \end{bmatrix}_m = I^{-1}\left\{ \begin{bmatrix} \bar{L} \\ \bar{M} \\ \bar{N} \end{bmatrix}_m - \begin{bmatrix} qr\left(I_z - I_y\right) - pqI_{xz} \\ rp\left(I_x - I_z\right) + \left(p^2 - r^2\right)I_{xz} \\ pq\left(I_y - I_x\right) + qrI_{xz} \end{bmatrix}_m \right\} \tag{20}$$

Substituting $I^{-1} = \begin{bmatrix} I_x & 0 & -I_{zx} \\ 0 & I_y & 0 \\ -I_{zx} & 0 & I_z \end{bmatrix}_m^{-1} = \frac{1}{I_y\left(I_x I_z - I_{zx}^2\right)}\begin{bmatrix} I_y I_z & 0 & I_y I_{zx} \\ 0 & I_x I_z - I_{zx}^2 & 0 \\ I_y I_{zx} & 0 & I_x I_y \end{bmatrix}_m$ gives:

$$\begin{bmatrix} \dot{p} \\ \dot{q} \\ \dot{r} \end{bmatrix}_m = \begin{bmatrix} \dfrac{-I_z^2 qr + I_z\left(\bar{L} + I_{zx}pq + I_y qr\right) + I_{zx}\left(\bar{N} + q\left(I_x p - I_y p - I_{zx} r\right)\right)}{I_x I_z - I_{zx}^2} \\ \dfrac{\bar{M} + \left(I_z - I_x\right)pr + I_{xx}\left(r^2 - p^2\right)}{I_y} \\ \dfrac{I_{zx}^2 pq + I_x\left(\bar{N} + \left(I_x - I_y\right)pq\right) + I_{zx}\left(\bar{L} - \left(I_x - I_y + I_z\right)qr\right)}{I_x I_z - I_{zx}^2} \end{bmatrix}_m \tag{21}$$

When the moving coordinate system is body coordinate system $O_b X_b Y_b Z_b$:

$$\begin{bmatrix} \dot{p} \\ \dot{q} \\ \dot{r} \end{bmatrix}_b = \begin{bmatrix} \dfrac{-I_z^2 qr + I_z\left(\bar{L} + I_{zx}pq + I_y qr\right) + I_{zx}\left(\bar{N} + q\left(I_x p - I_y p - I_{xx} r\right)\right)}{I_x I_z - I_{zx}^2} \\ \dfrac{\bar{M} + \left(I_z - I_x\right)pr + I_{zx}\left(r^2 - p^2\right)}{I_y} \\ \dfrac{I_{zx}^2 pq + I_x\left(\bar{N} + \left(I_x - I_y\right)pq\right) + I_{zx}\left(\bar{L} - \left(I_x - I_y + I_z\right)qr\right)}{I_x I_z - I_{zx}^2} \end{bmatrix}_b \tag{22}$$

The differential equation representing the position of the vehicle is:

$$\begin{bmatrix} \dot{x} \\ \dot{y} \\ \dot{z} \end{bmatrix}_g = \begin{bmatrix} \Delta\dot{N} \\ \Delta\dot{E} \\ -\Delta\dot{H} \end{bmatrix} = \begin{bmatrix} V_g \cos\gamma\cos\chi \\ V_g \cos\gamma\sin\chi \\ -V_g \sin\gamma \end{bmatrix} \tag{23}$$

Where N is the distance to the north relative to the origin of the ground coordinate system, E is the distance to the east relative to the ground coordinate system, and H is the vertical distance from the ground plane.

According to the definition, the relationship between Euler's angle and the angular velocity of rotation can be obtained as:

$$\begin{bmatrix} \dot{\phi} \\ \dot{\theta} \\ \dot{\psi} \end{bmatrix} = \begin{bmatrix} 1 & \sin\phi\tan\theta & \cos\phi\tan\theta \\ 0 & \cos\phi & -\sin\phi \\ 0 & \dfrac{\sin\phi}{\cos\theta} & \dfrac{\cos\phi}{\cos\theta} \end{bmatrix} \cdot \begin{bmatrix} p \\ q \\ r \end{bmatrix} \tag{24}$$

From the 12 differential equations and the necessary transformation matrices, the six-degree-of-freedom motion model of the vehicle in the body coordinate system is determined, and integrating these differential equations yields the 12 state variables of the vehicle motion.

2.2. Establishment of Virtual Cockpit 3D Model for General Purpose Vehicles

2.2.1. Virtual cockpit module realization scheme

This paper adopts the open-source flight simulation platform FlightGear, loads the three-dimensional model of the aircraft built by AC3d modeling software through the FlightGear simulation platform, and realizes the information interaction between the virtual cockpit and the other modules in the pilot training system through the self-developed communication program to achieve the virtual cockpit system that can provide virtual maneuvering training for pilots. The realization of the virtual cockpit system can be divided into the following steps:

(1) Establish the 3D model of the cockpit. Including the aircraft appearance model, instrument model, various buttons and joystick model;

(2) Write the driver file of the cockpit model, which is the xml format configuration file supported by FlightGear simulation platform and the Nasal scripting language that defines various actions of the aircraft;

(3) Develop the communication software of the virtual cockpit to realize the information interaction between the cockpit and other modules in the pilot training system.

The realization process of the virtual cockpit system is shown in Figure 2.

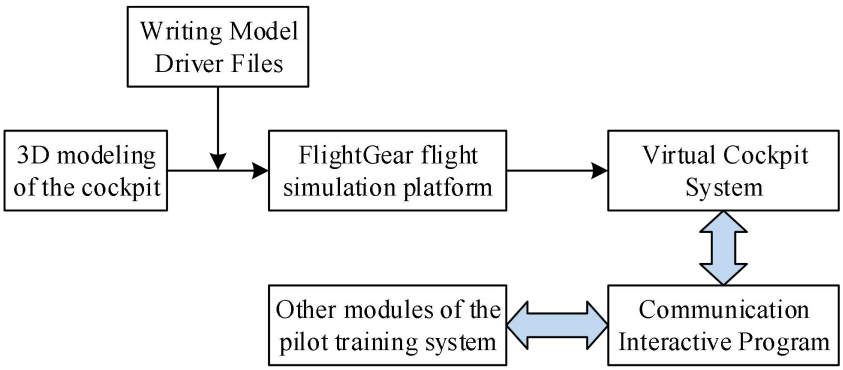

Figure 2. Implementation process of the virtual cockpit system.

2.2.2. Regular Geometry Modeling

Modeling using modern computer graphics technology, there are mainly the following three commonly used methods:

(1) Purely manual modeling and programming methods, the spatial coordinates of the model are calculated manually by the programmer, and the shape and parameters of the model's facets are programmed by the programmer and saved as a model file. When using the model, OpenGL is used to read the file and display the image to the user in real time. Although this method does not require other modeling platform software, its modeling process is very cumbersome and requires rich modeling experience and high level of three-dimensional mathematics, obviously, this method is not suitable for the modeling of virtual cockpit systems.

(2) Adopt commercial modeling software, which is powerful and friendly. For developing cockpit models, commercial modeling software can improve the efficiency of the project.

(3) Secondary development, the use of commonly used secondary development language, through programming to achieve roughly the same parameters, the shape of a more regular model modeling development, the model through the programming of automated batch processing to achieve, is a more efficient way. This has a great role in the development of the virtual cockpit system.

Combined with the characteristics of the regular model in the virtual cockpit system, the above three modeling methods have the following applications in virtual cockpit modeling:

(1) The first modeling method can be used to establish certain detail parts in the cockpit, whose modeling is easier to implement and has greater independence in the cockpit model, and can be combined with the OpenGL graphics language to implement the scene drawing part with callback functions.

(2) The second method is suitable for modeling most of the regular models in the virtual cockpit, using mature commercial modeling software to model complex models with shape and structure, thus making model development easy to implement and giving full play to the advantages of commercial modeling software in terms of model database format.

(3) Within the virtual cockpit scene, the third modeling method is used for object models with consistent appearance and similar structure.

2.3. The construction of the human balance perception ability detection platform

2.3.1. Measurement of human balance perception ability

In this paper, we propose a human balance perception ability measurement method to analyze the influence of sensory organs on balance ability, assess the balance perception ability of subjects, and then diagnose whether the balance perception ability of patients with balance disorders is reduced or not, as well as the influence of sensory organs on balance disorders.

In order to minimize the differences in the limb movement system, this testing platform needs to provide a specific device to replace the subject's limb movement. Subjects control the device by using a joystick to swing it in two directions: forward and backward, left and right. Under different balance conditions, the subject's balance perception ability is determined by measuring the balance angle of the subject's controlled movement of the device.

During the measurement, the test platform adopts the control variable method to adjust the visual, somatosensory and vestibular organ position sensory information, so that the subject is in different sensory information scenes. The sensory information scenarios were categorized into eight categories

according to the effectiveness of the sensory information.

2.3.2. Testing platform implementation program

The test platform is divided into two parts, the upper part to realize the replacement of the subject's limb balance movement, and the lower part to provide a horizontal angle can be controlled tilt movement environment. The upper part of the test platform adopts two electric actuators to realize the adjustment of the pitch and roll angles, and the subject swings backward and forward, left and right instead of his/her limb movement through the rocker control during the test; the lower part of the test platform adopts a heavy-duty electric actuator to provide the balance movement environment of the upper part of the test platform. According to the direction of the subject's sitting posture, the balance test can be carried out in the corresponding direction.

The data acquisition module adopts two gyroscopes to collect the horizontal angle of the upper and lower parts of the testing platform, and the balance control of the upper part is carried out through the rocker; the USART serial port is used to communicate with the computer to realize the selection of test modes of the testing platform and the storage of experimental data. The overall function of the testing platform is shown in Figure 3.

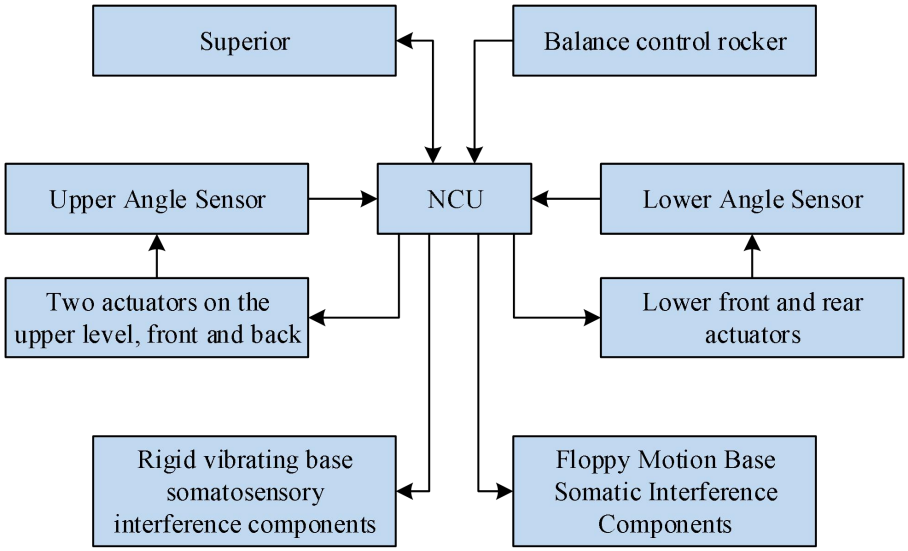

Figure 3. The overall functional framework of the detection platform.

Studies have shown that eyelid closure during standing increases muscle excitation and affects postural control. Referring to the methods of existing studies, it was determined that the visual information was controlled by an opaque eyecup.

Since somatosensation is closely related to human limb movement, there is a high degree of coupling between somatosensory deep sensation and balance control. Therefore, a straitjacket was used to restrict the limb movement in the seated state of the subject and inhibit the generation of proprioception. To determine the control mode of somatosensory information: the use of hard vibration and soft and up and down motion adjustable cushions to provide four kinds of somatosensory information: hard base, hard vibration base, soft base and soft motion base; to determine the control mode of vestibular position information: the use of the neck brace to fix the head to achieve the vertical position of the head and head lateral tilt position adjustment.

3. Analysis of the impact of virtual reality technology on the training of pilots' balance perception skills

3.1. Virtual Cockpit Tracking Performance Testing

To test the tracking performance of the virtual cockpit of the vehicle in this paper, the pixel difference between the hand region in the horizontal and vertical directions and the actual position of the hand during the tracking process is used as the tracking accuracy measure. The experimental result error is shown in Fig. 4, with the horizontal axis indicating the current number of tracking frames. Since different gesture sequences contain different numbers of frames, this paper is unable to draw a motion tracking

error map containing all the gesture sequences, so this paper only shows the mean value information of the video sequence error for about 100 frames in the error map. It can be seen that both horizontal and vertical hand deviations during hand tracking are within 5 pixel points.

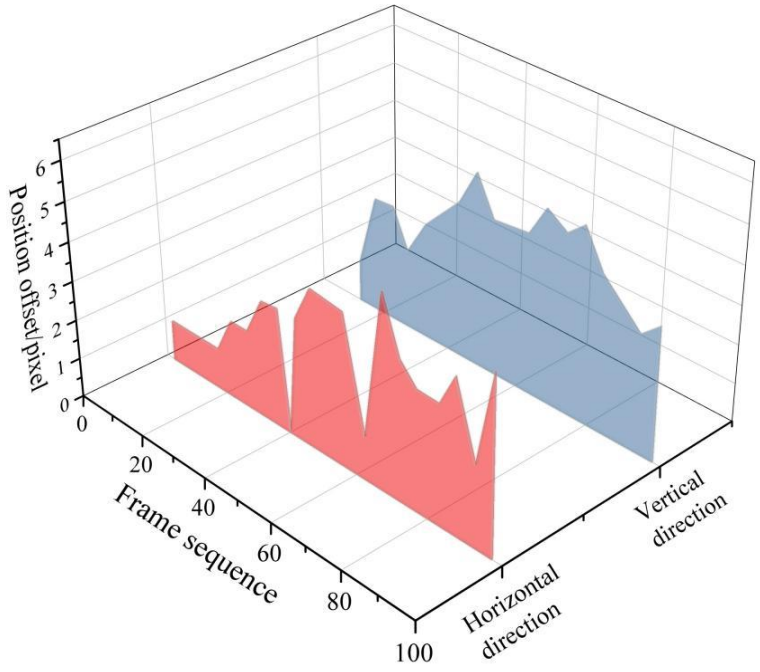

Figure 4. Error of experimental results.

3.2. Pilot Balance Perception Ability Tests

The 156 pilots who were hospitalized for modified physical examination and concluded as flight qualified from October 2024 to December 2024, aged 23 to 39 years old, with a flight time of 300 to 3800 h, were used as the study subjects. 89 of them were male and 67 were female. Inclusion criteria: (1) bachelor's degree; (2) right-handed and normal vision; (3) able to operate the handle skillfully; (4) no sense of vertigo when wearing the helmet; (5) listening to the test arrangements, with a positive attitude, and actively cooperating with the completion of the tests; (6) all of them voluntarily participated in the test and signed the informed consent form.

The Pilot Technical Proficiency Test is conducted in a quiet environment and consists of a 30-item scale designed to assess as objectively as possible the actual flying ability of the pilot. Pilots are evaluated on the basis of their actual skill level and the items in the scale, using a five-point scale, objectively and accurately. The pilots were grouped according to the total score of the scale in accordance with the principle of 27% distribution, and the first 27% of the total score in descending order were regarded as the high spatial ability group (42 cases), the last 27% were regarded as the low spatial ability group (42 cases), and the rest were regarded as the medium spatial ability group (72 cases). There was no significant difference (P>0.05) among the three groups of pilots in terms of age, gender and flight time, and the results of the comparison of the general information of the pilots in different spatial ability groups are shown in Table 1. There were no significant differences in age (F=3.014, P=0.061), gender (χ^2=1.642, P=0.507), and flight time (F=2.084, P=0.156) in the three groups, and the groups were comparable.

Table 1. Comparison results of general information of pilots.

Group	Age	Gender		Flight time/h
		Male (n=89)	Female (n= 67)	
High spatial ability group	32.53±6.38	29	13	1429.45±983.11
Medium spatial	29.04±6.05	34	38	1048.17±964.48

ability group				
Low spatial ability group	28.17±6.01	26	16	951.37±972.27
F/χ^2	3.014	1.642		2.084
P	0.061	0.507		0.156

The differences in the balance perception ability test of pilots from different spatial ability groups are shown in Table 2. By statistically analyzing the balance perception ability test of pilots in different spatial ability groups, the results suggest that the pilots in the high spatial ability group, medium spatial ability group and low spatial ability group have significant differences in the balance perception ability test in terms of reaction time (H=6.947, P=0.031), the number of correct per unit of time (H=6.932, P=0.025), and the rate of correctness (H= 0.419, P=0.726) did not differ.

Table 2. Differences in test results among different spatial ability groups.

Group	Response time (s)	Accuracy rate	Number of correct items per unit time (items/s)
High spatial ability group	319.7 (259.6,451.9)	0.731 (0.70,0.74)	0.112 (0.08,0.16)
Medium spatial ability group	371.4 (284.7,488.1)	0.768 (0.68.0.83)	0.101 (0.07,0.14)
Low spatial ability group	441.2 (304.3.548.9)	0.742 (0.68,0.87)	0.089 (0.07,0.11)
H	6.947	0.419	6.932
P	0.031	0.726	0.025

The differences in the balance perception ability test of pilots of different genders are shown in Table 3. After statistically analyzing the balance perception ability test of pilots of different genders, it was found that there was no statistical difference between male and female pilots in terms of reaction time, correct rate and number correct per unit of time in the balance perception ability test (P>0.05).

Table 3. Differences in test results between male and female pilots.

Project	Male (n=89)	Female (n=67)	F/(Z)	P
Age	29.92±6.573	29.51±4.368	3.972	0.029
Flight time (h)	1142.50±983.58	1099.03±936.31	5.018	0.031
Response time (s)	374.9 (312.4,498.3)	378.04 (371.3,523.2)	(-1.229)	0.206
Accuracy rate	0.748 (0.681,0.802)	0.755 (0.761,0.814)	(-0.021)	0.894
Number of correct items per unit time (items/s)	0.101 (0.08,0.13)	0.100 (0.07,0.12)	(-1.243)	0.311

3.3. Impact analysis

To investigate the practical usefulness of the virtual reality-based flight cockpit in the training of pilots' balance perception ability in this paper, a controlled experiment was designed and implemented. The subjects of the experiment were 156 active pilots who were hospitalized for a modified physical examination between October and December 2024 and whose physical examination concluded that they were flight-qualified. After completing a baseline assessment of a standardized set of balance perception ability tests, all pilots were subsequently divided into experimental and control groups on a randomized

grouping basis, where the experimental group was given a virtual reality-based immersive balance perception training module added to the standard training, while the control group received only basic simulator training. The training period was 4 weeks, with 3 training sessions per week, each lasting about 30 minutes. At the end of the training, all subjects received the same balance perception ability test again, and the effect of virtual reality technology on pilots' balance perception ability training was assessed by comparing the differences in each index between the two groups before and after the experiment.

3.3.1. Reaction time

The results of the comparison of the reaction time test data of the two groups before and after the experiment are shown in Figure 5 (a~b). The mean data obtained from the reaction time test of the experimental group after the experiment decreased by 49.3s, with a drop of 13.1%, and the p-value of the T-test of the matched samples within the group was 0.00, which was less than 0.05, and the test result was a significant difference, indicating that the reaction time level of the experimental group had a great progress after the 4-week training of balance ability under the simulation of the virtual reality technology in the group. The mean data obtained from the reaction time test of the control group decreased by 18.5s, or 4.9%, and the p-value of the matched samples t-test within the group was 0.00, which was less than 0.05, and the test result was a significant difference, which indicates that the reaction time of the control group also decreased to a certain extent after the 4-week training of general balance ability. An independent samples t-test between the groups after the experiment yielded a p-value of 0.024, which is less than 0.05 and is significantly different.

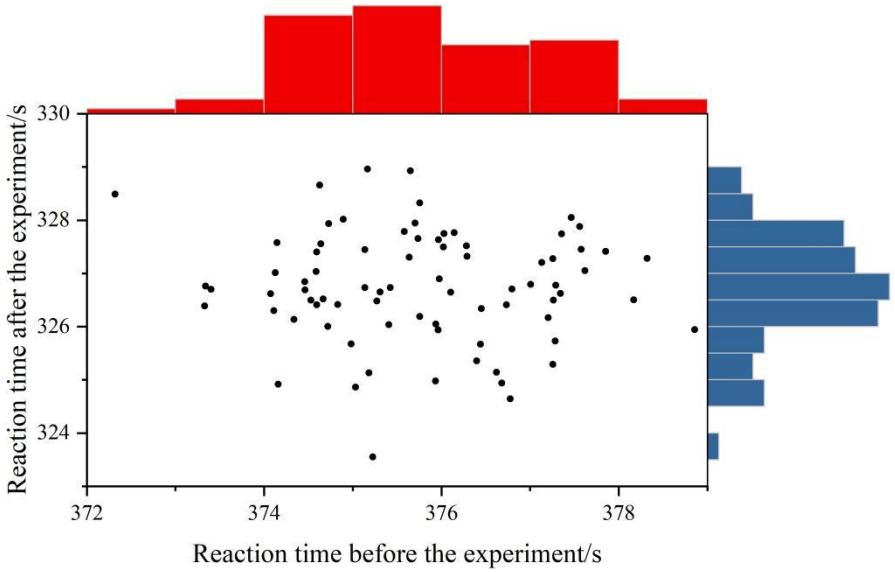

(a) Experimental group

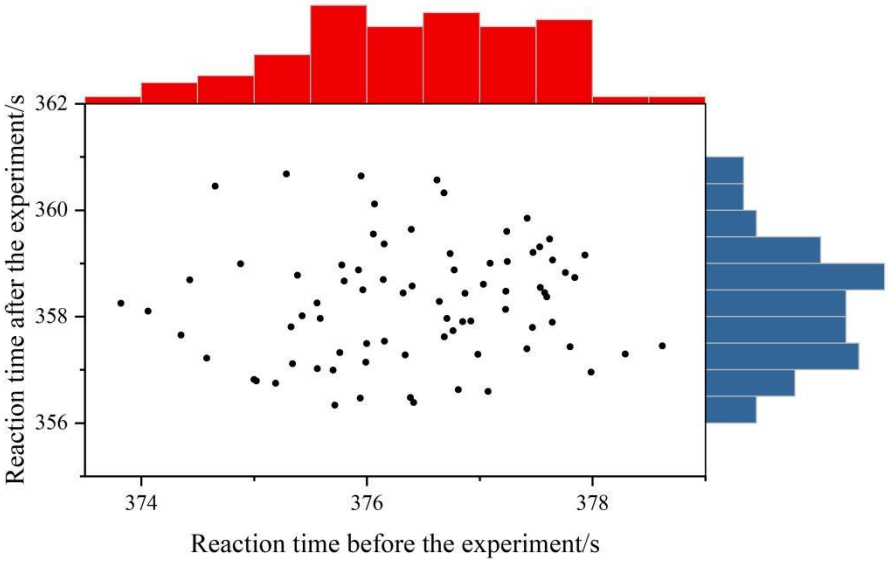

(b) Control group

Figure 5. Comparison results of reaction time test data.

3.3.2. Correctness

The results of the comparison of the correctness test data between the two groups before and after the experiment are shown in Fig. 6 (a~b). The mean data obtained from the correctness test of the experimental group after training increased by 0.06, an increase of 8.0%. The matched-sample t-test within the group shows that the p-value is 0.00, which is less than 0.01, and the test result shows that there is a very significant difference, thus proving that the experimental group has a great improvement in the dynamic balance ability of the correctness test in the experimental group after a 4-week training of the balance ability in the simulation of virtual reality technology. The mean data from the correctness test of the control group increased by 0.038, or 5.1%, and a matched-sample t-test within the group yielded a p-value of 0.001, which is less than 0.01, and the result of the test was that there was a highly significant difference. An independent samples t-test conducted after training between the experimental and control groups yielded a p-value of 0.197, which is greater than 0.05, meaning that there is no significant difference. The test results indicate that there is no significant difference in reaction time between the two groups after training. It can be seen that both the experimental group trained with VR and the control group trained without VR resulted in an increase in the correctness of the pilots and the increase in the experimental group with VR was greater than that of the control group by 2.9%.

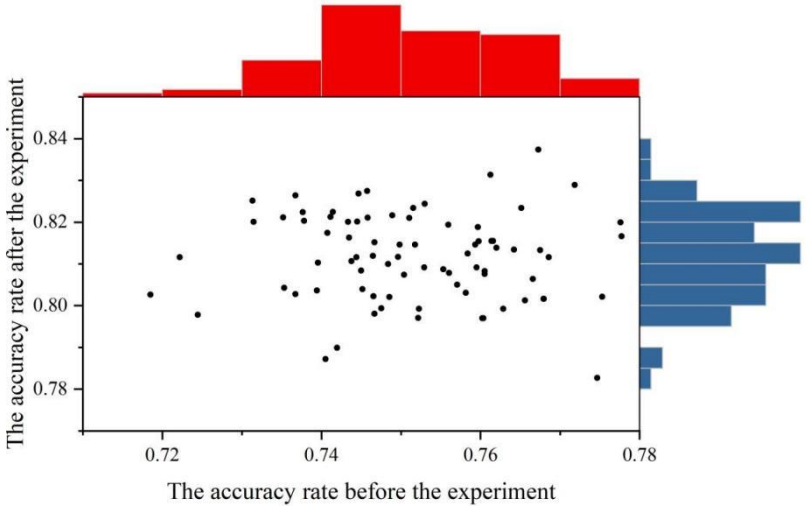

(a) Experimental group

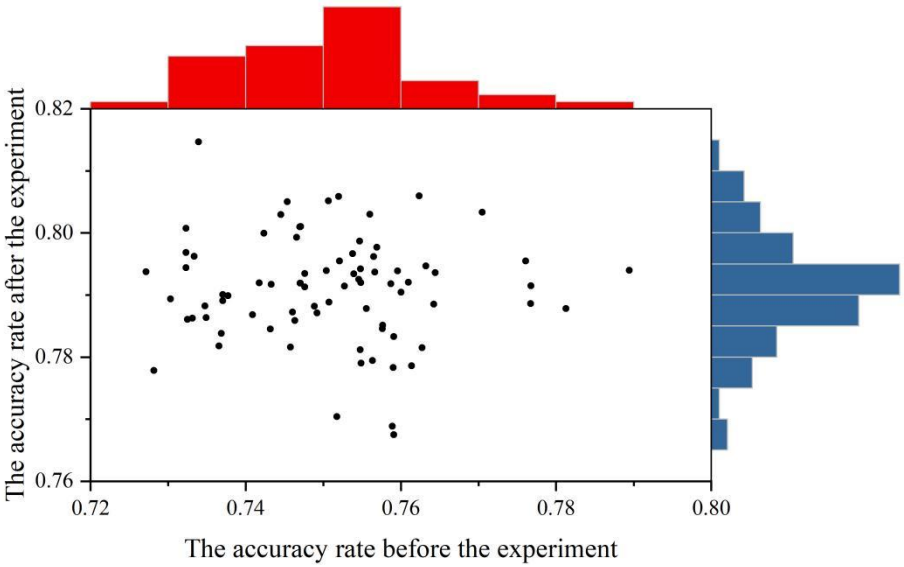

(b) Control group

Figure 6. Comparison results of accuracy test data.

3.3.3. Correct number per unit time

The results of the comparison of the number correct per unit time test data between the two groups before and after the experiment are shown in Figure 7 (a~b). The average value of the number of correct unit time tests of the experimental group after training increased by 0.017 per second, an increase of 17.2%, and the matched-sample t-test of the group yielded a p-value of 0.00, which is less than 0.01, and the test result is that there is a very significant difference, which proves that the experimental group's level of the correct number of correct unit time tests of the experimental group after a 4-week training of the balancing ability under the simulation of the virtual reality technology had a Significantly improved. In the control group, the mean value of the number of correct units per second increased by 0.006 units per second, an increase of 5.9%, and the p-value of the matched samples t-test within the group was 0.00, which is less than 0.01, and the result of the test was that there was a very significant difference, which indicates that the number of correct units per second of the control group also had a certain degree of progress after a 4-week training of the general balancing ability. The p-value after independent samples t-test between the groups after training was 0.019, which is less than 0.05, i.e. there is a significant difference.

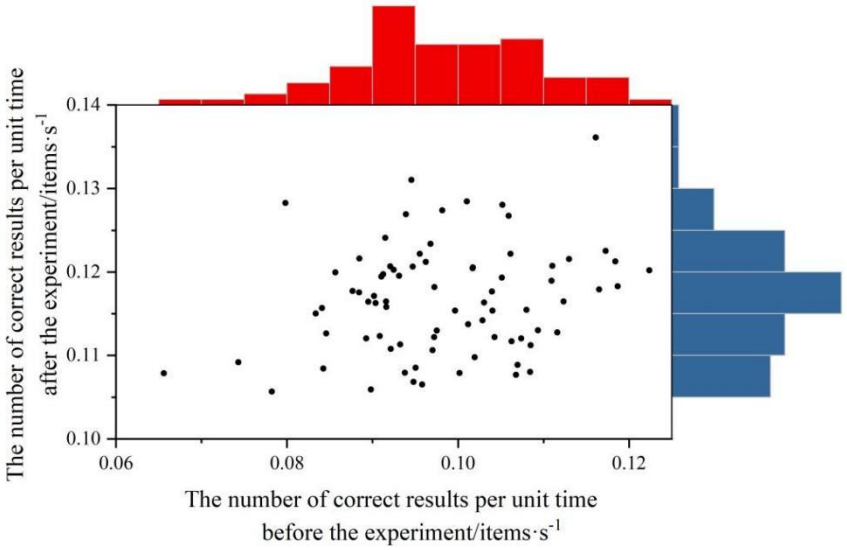

(a) Experimental group

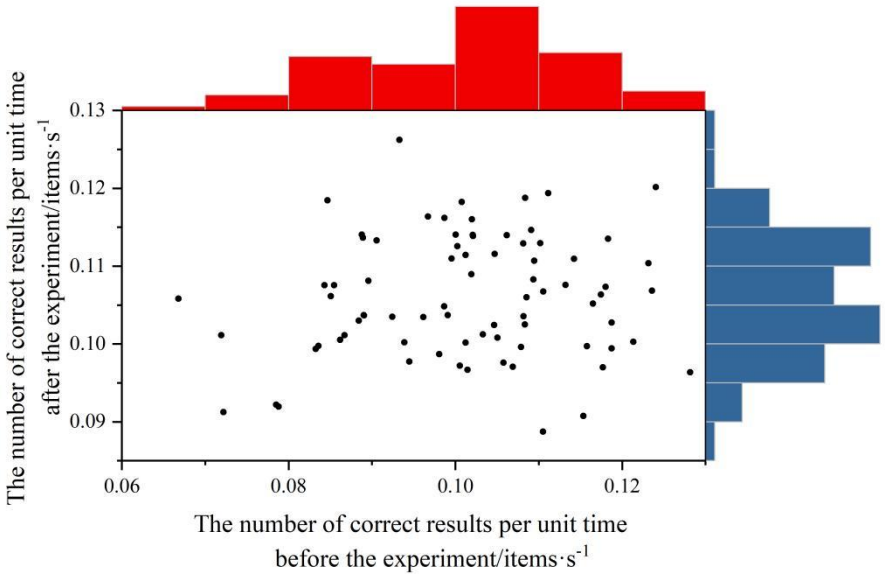

(b) Control group

Figure 7. Comparison results of correct numbers over unit time test data.

4. Conclusion

This paper designs and develops a 3D visualization cockpit system capable of providing flight maneuvering training to explore how balance training under virtual reality technology simulation differs from general balance training in a conventional state.

In the experimental group, the mean data from the reaction time test decreased by 49.3s after the experiment, a decrease of 13.1%, and the p-value of the matched-sample t-test within the group was 0.00, which was less than 0.05, and the test result was a significant difference. The mean data obtained from the reaction time test for the control group decreased by 18.5s, a decrease of 4.9%, with a p-value of 0.00, less than 0.05, for the within-group matched samples t-test, which resulted in a significant difference. An independent samples t-test between the groups after the experiment yielded a p-value of 0.024, which is less than 0.05 and significantly different.

The mean data obtained from the post-training correctness test for the experimental group increased by 0.06, an increase of 8.0%. A matched samples t-test within the group shows a p-value of 0.00, which is less than 0.01, and the test shows a highly significant difference. The mean data obtained from the correctness test for the control group increased by 0.038, an increase of 5.1%, and a matched samples t-test within the group yielded a p-value of 0.001, which is less than 0.01, and the test showed a highly significant difference. An independent samples t-test conducted after training between the experimental and control groups yielded a p-value of 0.197, which is greater than 0.05, meaning that there is no significant difference. Both the experimental group trained with VR and the control group trained without VR resulted in an increase in the correctness of the pilots and the increase in the experimental group with VR was greater than the 2.9% increase in the control group.

The mean number of correct tests per unit of time for the experimental group increased by 0.017 correct tests per unit of time after training, an increase of 17.2%, and a matched samples t-test within the group yielded a p-value of 0.00, which is less than 0.01, and the test result is a very significant difference. The control group's mean value for the number correct per unit time test increased by 0.006 per second, an increase of 5.9%, and a matched samples t-test within the group yielded a p-value of 0.00, which is less than 0.01, and the test result was a very significant difference. The p-value after independent samples t-test between groups after training was 0.019, which is less than 0.05, which means that there is a significant difference.

The significant difference between the reaction time and the number of correct units of time between the experimental and control groups in the experiment corroborates that the use of virtual reality technology helps to optimize the efficiency of the pilot's multimodal information integration, which further affects the pilot's balance perception ability.

Funding
This paper was supported by:
China Institute of Communications Education: “Research on Development Trends and Innovative Models of Physical Education Curriculum for Civil Aviation Flight Cadets Under the Guidance of Xi JinPing's Sports-Related Discourse” (NO: JT2024ZD094);
The Fundamental Research Funds for the Central Universities: “An Empirical Study on Integrating Physical Fitness into University Physical Education Curriculum Under the Lifelong Sports Concept” (NO:3122025007).

References

1. van Weelden, E., Alimardani, M., Wiltshire, T. J., & Louwerse, M. M. (2021, September). Advancing the adoption of virtual reality and neurotechnology to improve flight training. In 2021 IEEE 2nd International Conference on Human-Machine Systems (ICHMS) (pp. 1-4). IEEE.
2. Fussell, S. G., & Truong, D. (2020). Preliminary results of a study investigating aviation student’s intentions to use virtual reality for flight training. International Journal of Aviation, Aeronautics, and Aerospace, 7(3), 2.
3. Bauer, M., & Klingauf, U. (2008). Virtual-reality as a future training medium for civilian flight procedure training. In AIAA modeling and simulation technologies conference and exhibit (p. 7030).
4. Oh, C. G. (2020, December). Pros and cons of a VR-based flight training simulator; empirical evaluations by student and instructor pilots. In Proceedings of the human factors and ergonomics society annual meeting (Vol. 64, No. 1, pp. 193-197). Sage CA: Los Angeles, CA: SAGE Publications.
5. Zeng, C., Chen, X., Ge, Z., Wang, Y., Cao, W., & Zhang, C. (2023, September). An exploration of final flight training based on virtual reality technology. In 2023 International Conference on Computer Applications Technology (CCAT) (pp. 287-290). IEEE.
6. Li, S. (2023). Design and development of aviation aircraft maintenance training platform based on VR technology. Procedia Computer Science, 228, 898-906.
7. Cross, J. I., & Ryley, T. (2025). Assessing evidence-based training in a collaborative virtual reality flight simulator. The Aeronautical Journal, 129(1332), 261-281.
8. Somerville, A., Joiner, K., Lynar, T., & Wild, G. (2025). Applications of extended reality in pilot flight simulator training: a systematic review with meta-analysis. Visual Computing for Industry, Biomedicine, and Art, 8(1), 1-30.
9. Oberhauser, M., & Dreyer, D. (2017). A virtual reality flight simulator for human factors engineering. Cognition, Technology & Work, 19(2), 263-277.
10. Lee, A. T. (2017). Flight simulation: virtual environments in aviation. Routledge.
11. Somerville, A., Joiner, K., & Wild, G. (2025). Effects of Flight Experience or Simulator Exposure on Simulator Sickness in Virtual Reality Flight Simulation. Multimodal Technologies and Interaction, 9(3), 24.
12. Li, L., Chen, Y., & Xing, R. (2025). Influence and mechanism of resilience on flight operational performance under different flight situations: A study based on flight simulator experiments. Safety Science, 184, 106763.
13. Rostami, M., Kamoonpuri, J., Pradhan, P., & Chung, J. (2023). Development and evaluation of an enhanced virtual reality flight simulation tool for airships. Aerospace, 10(5), 457.
14. Ross, G., & Gilbey, A. (2023). Extended reality (xR) flight simulators as an adjunct to traditional flight training methods: a scoping review. CEAS Aeronautical Journal, 14(4), 799-815.
15. Cross, J. I., & Boag-Hodgson, C. C. (2025). A Collaborative Virtual Reality Flight Simulator: Efficacy, Challenges and Potential. IEEE Transactions on Learning Technologies.
16. Zhao, K. R., Xu, S., Ye, Q., & Li, Y. (2011, May). Design and realization of flight simulation system based on virtual reality technology. In 2011 Chinese Control and Decision Conference (CCDC) (pp. 4361-4364). IEEE.
17. Auer, S., Gerken, J., Reiterer, H., & Jetter, H. C. (2021). Comparison between virtual reality and physical flight simulators for cockpit familiarization. In Proceedings of Mensch Und Computer 2021 (pp. 378-392).
18. Guthridge, R., & Clinton-Lisell, V. (2023). Evaluating the efficacy of virtual reality (VR) training devices for pilot training. Journal of Aviation Technology and Engineering, 12(2), 1.
19. Rizvi, S. A., Rehman, U., Cao, S., & Moncion, B. (2025). Exploring technology acceptance of flight simulation training devices and augmented reality in general aviation pilot training. Scientific Reports, 15(1), 2302.
20. Fiorillo, V., Martino, B., Castelli, V., Filipponi, E., Braga, L., Randolfi, A., ... & Di Berardino, F. (2025). Postural Balance in Italian Air Force Pilots: Development of Specific Normative Values. Audiology Research, 15(3), 70.